Kinetics and Optimization Studies of Modified VPO/γ-Al_2O_3 Catalyst Prepared In situ for Cross-aldol Condensation

Hui Guo[1], Tingting Ge[1,*], Yuchao Li[1], Yuxia Li[1], Yanxia Zheng[1], Xinpeng Guo[2], Haofei Huang[1], Ming Wang[1], Cuncun Zuo[1,*]

[1] Institute of Clean Chemical Technology, School of Chemistry and Chemical Engineering, Shandong University of Technology, Zibo 255000, People's Republic of China

[2] National & Local United Engineering Research Center for Chemical Process Simulation and Intensification, School of Chemical Engineering, Xiangtan University, Xiangtan 411105, People's Republic of China

*Corresponding author: Cuncun Zuo. TEL/FAX: +86-0533-2781664; E-mail: zcc_xtu@163.com

Tingting Ge. TEL/FAX: +86-0533-2781664; E-mail: gtt_swpu@163.com

Results and Discussion

Materials characterization

Table S1 The crystallite size of catalyst with different active component loadings.

catalyst	average crystal size (nm)	
	$(VO)_2P_2O_7$	$AlPO_4$
20%VPO/γ-Al_2O_3	17.4	26.7
40%VPO/γ-Al_2O_3	17.6	24.1
50%VPO/γ-Al_2O_3	18.1	23.6
60%VPO/γ-Al_2O_3	18.3	23.4
80%VPO/γ-Al_2O_3	21.5	35.6

Table S2 The crystallite size of catalyst with different calcination temperatures.

catalyst	average crystal size (nm)		
	$(VO)_2P_2O_7$	$VOPO_4$	$AlPO_4$
60%VPO/γ-Al_2O_3-270°C	17.4	19.6	26.7
60%VPO/γ-Al_2O_3-300°C	17.6	17.8	24.1
60%VPO/γ-Al_2O_3-350°C	18.1	16.4	23.6
60%VPO/γ-Al_2O_3-450°C	18.3	20.1	23.4

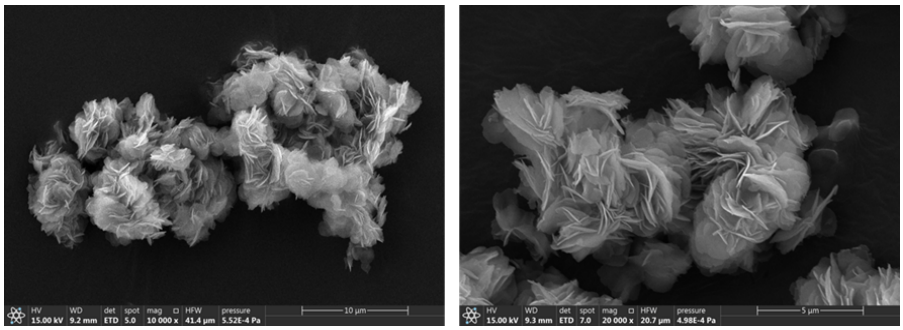

Figure S1 The SEM images of VPO catalyst.

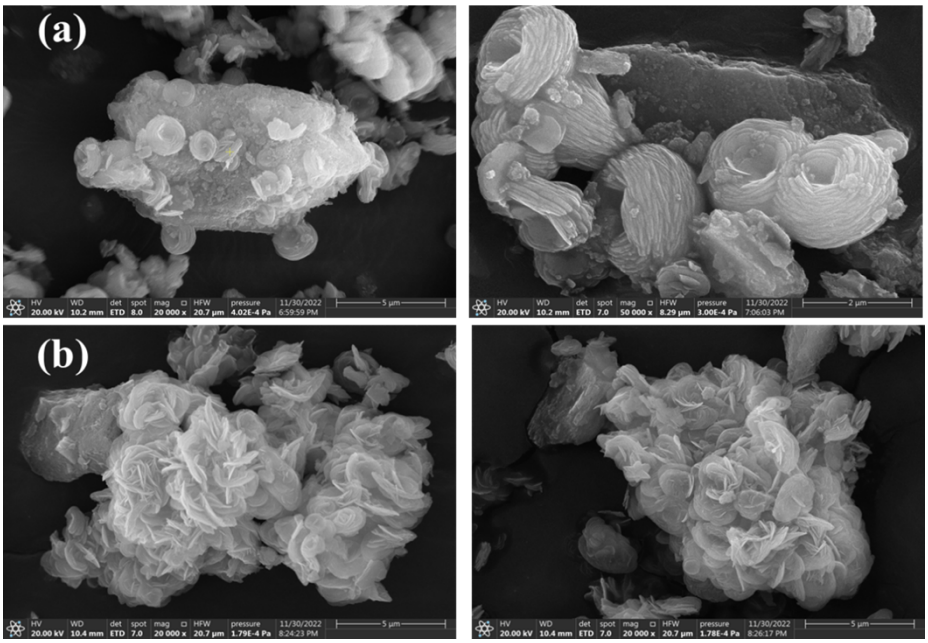

Figure S2 The SEM images of (a) 20% VPO/γ-Al_2O_3 and 80% VPO/γ-Al_2O_3 catalyst.

Table S3 The amounts of acid and base sites of the VPO/γ-Al_2O_3 catalysts with different calcination temperature and different active component loadings.

Catalyst	Weak basic sites (mmol/m^2)	Medium-strong acidic sites (mmol/m^2)
270℃-60%VPO/γ-Al_2O_3	0.0215	0.0227
350℃-60%VPO/γ-Al_2O_3	0.0254	0.0265
450℃-60%VPO/γ-Al_2O_3	0.0250	0.0259
350℃-40%VPO/γ-Al_2O_3	0.0241	0.0245
350℃-80%VPO/γ-Al_2O_3	0.0256	0.0266

Table S4 Basic parameters of IR absorption peaks at about 3450 cm^{-1} and 1600 cm^{-1} for VPO/γ-Al_2O_3 catalysts with different active component loadings.

catalyst	3450cm^{-1}(H-OH)			1600cm^{-1}(H-OH)		
	Peak height	Peak area	FWHM	Peak height	Peak area	FWHM
20%VPO/γ-Al_2O_3	34.61	25730.85	701.07	12.12	911.03	71.86
40%VPO/γ-Al_2O_3	37.54	28174.61	649.53	13.64	949.50	74.47
60%VPO/γ-Al_2O_3	42.12	33699.10	687.46	17.56	1313.92	85.26
80%VPO/γ-Al_2O_3	40.60	30186.42	714.28	15.09	1112.81	87.75

Table S5 CO_2 desorption temperature of catalysts with different active component loadings.

Catalyst	Temperature of the desorption peak (℃)
40%VPO/γ-Al_2O_3	113.2
60%VPO/γ-Al_2O_3	102.4
80%VPO/γ-Al_2O_3	91.7

The results of ICP analysis of VPO/Al_2O_3 catalysts were shown in Table S6. The elemental contents of V, P, and Al in the used VPO/γ-Al_2O_3 catalyst were similar to those in the fresh catalyst. It indicated that the catalyst components were not lost during the reaction process.

Table S6 Estimation of V, P, Al contents from ICP-OES in 60%VPO/Al_2O_3 catalyst.

Catalyst	Test items	Fresh catalyst	Used catalyst
60%VPO/γ-Al_2O_3	V	16.5%	16.5%
	P	12.1%	12.0%
	Al	26.8%	26.5%

Response surface analysis

Table S7 The experimental design and response values.

Run	Factor 1 A:Molar ratio	Factor 2 B:Temperature ℃	Factor 3 C:Space velocity h^{-1}	Response 1
1	5	350	1.2	52.21
2	5	330	1.6	32.74
3	7	350	0.8	47.21
4	3	350	0.8	42.27
5	3	350	1.6	40.52
6	5	370	1.6	31.17
7	5	350	1.2	52.14
8	5	350	1.2	51.85
9	3	370	1.2	26.74
10	5	370	0.8	31.74
11	5	350	1.2	52.05
12	7	330	1.2	33.44
13	3	330	1.2	29.54
14	5	330	0.8	36.72
15	5	350	1.2	52.37
16	7	370	1.2	30.55
17	7	350	1.6	44.71

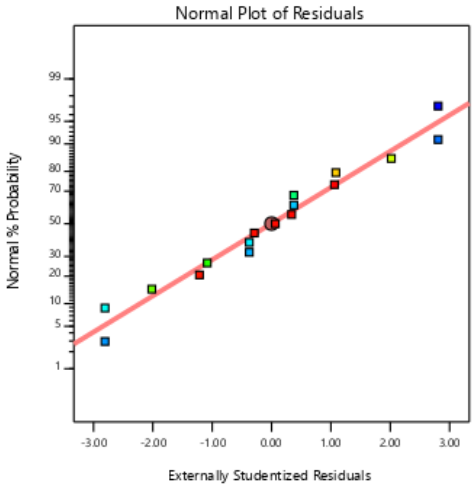

Figure S3 Normal probability plot.

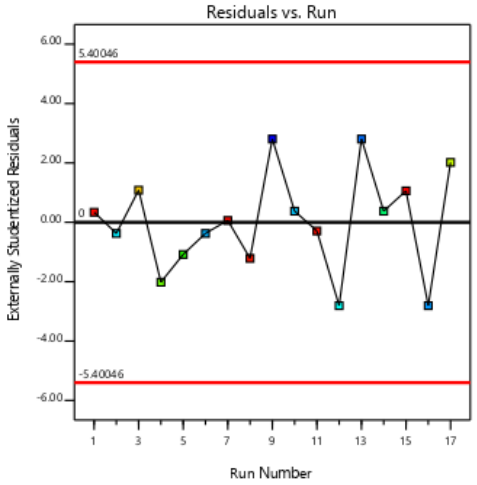

Figure S4 Run order residual plot.

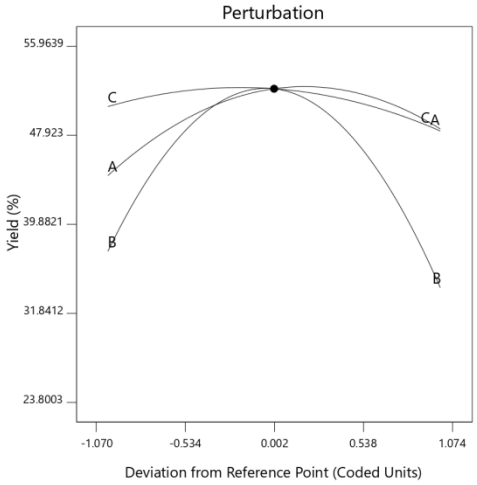

Figure S5 Perturbation curve.

Aldol condensation reaction kinetics

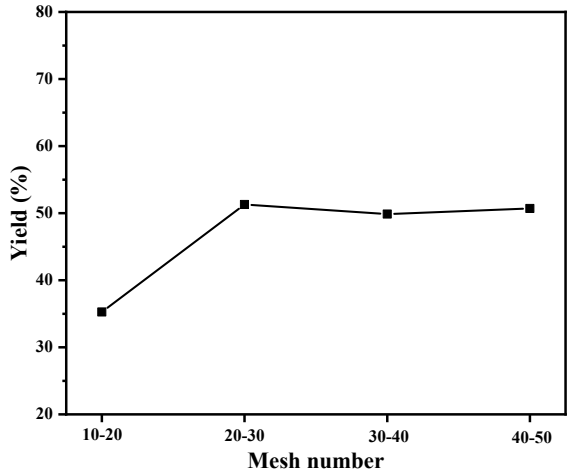

Figure S6 Effect of catalyst particle size on catalytic performance.

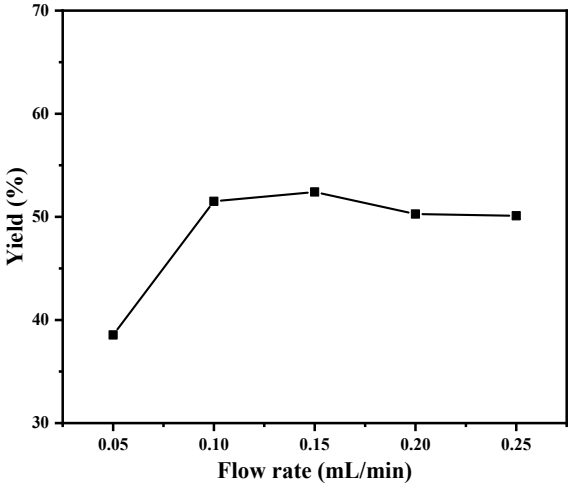

Figure S7 Effect of flow rate on catalytic performance.

Figure S6 showed the effect of catalyst size on the performance of the reaction, with the yield of AA remaining essentially constant for catalyst sizes d>20 mesh. It is suggested that the effect of catalyst particle size on internal diffusion can be eliminated for catalyst particle sizes d>20 mesh. The effect of different flow rate on the yield of AA was investigated in Figure S7 AA yield remained constant at feed flow rate above 0.1 mL/min, which eliminated the effect of external diffusion on aldol condensation reaction.

Table S8 Variation of HCHO concentration with reaction time at different temperature.

LHSV (h^{-1})	Reaction time (min)	C_{HCHO} (603 K)	C_{HCHO} (623 K)	C_{HCHO} (643 K)	C_{HCHO} (663 K)
1.5	40	1.550	1.358	1.205	1.112
1.7	35	1.663	1.483	1.330	1.260
2	30	1.794	1.618	1.465	1.395
2.4	25	1.912	1.778	1.645	1.555
3	20	2.087	1.974	1.849	1.790

Table S9 Values and correlations of the parameters in the fitted equation.

	y_0	A_1	t_1	R^2
603 K	0.72840	2.22490	40.27950	0.998
623 K	0.67265	2.45744	31.40538	0.999
643 K	0.60738	2.57653	27.41172	0.999
663 K	0.50863	2.65359	27.28710	0.997

Table. S10 Values and correlations of the parameters in the fitted equation.

	lnk	α	R^2
603 K	-4.6243	1.6866	0.997
623 K	-4.3366	1.7103	0.998
643 K	-4.1290	1.7047	0.997
663 K	-3.9623	1.5715	0.997

The effect of reaction temperature (330-390 °C) and space velocity on aldil condensation reaction was studied in a fixed bed reactor and the variation of HCHO concentration at different reaction time is shown in Table S2. Table S3 demonstrated the parameters of the equation and their correlation coefficients after fitting the equation to $C_{HCHO} \sim t$ at different temperature. Table S4 showed the parameters of the equation and their correlation coefficients after fitting the equation to $\ln C_{HCHO} \sim \ln r_A$ at different temperature.